Journal of Pathology
J Pathol May 2021; **254:** 46–56
Published online 19 February 2021 in Wiley Online Library (wileyonlinelibrary.com) DOI: 10.1002/path.5630

ORIGINAL PAPER

Cellular and physical microenvironments regulate the aggressiveness and sunitinib chemosensitivity of clear cell renal cell carcinoma

Kei Nagase[1,2*], Takashi Akutagawa[1], Mihoko Rikitake-Yamamoto[1], Sayuri Morito[1], Maki Futamata[1], Shohei Tobu[2], Mitsuru Noguchi[2], Shuji Toda[1] and Shigehisa Aoki[1*]

[1] *Division of Pathology, Department of Pathology and Microbiology, Faculty of Medicine, Saga University, Saga, Japan*
[2] *Department of Urology, Faculty of Medicine, Saga University, Saga, Japan*

**Correspondence to: K Nagase or S Aoki, Division of Pathology, Department of Pathology and Microbiology, Faculty of Medicine, Saga University, 5-1-1 Nabeshima, Saga 849-8501, Japan. E-mail: kei.nagase.1007@gmail.com; aokis@cc.saga-u.ac.jp*

The copyright line for this article was changed on 10 April 2021 after original online publication.

Abstract

Renal cell carcinoma (RCC) is the most predominant type of kidney cancer in adults and is responsible for approximately 85% of clinical cases. The tumor–specific microenvironment includes both cellular and physical factors, and it regulates the homeostasis and function of cancer cells. Perirenal adipose tissue and tumor–associated macrophages are the major cellular components of the RCC microenvironment. The RCC microvasculature network generates interstitial fluid flow, which is the movement of fluid through the extracellular compartments of tissues. This fluid flow is a specific physical characteristic of the microenvironment of RCC. We hypothesized that there may be an interaction between the cellular and physical microenvironments and that these two factors may play an important role in regulating the behavior of RCC. To elucidate the effects of adipose tissue, macrophages, and fluid flow stimulation on RCC and to investigate the relationships between these factors, we used a collagen gel culture method to generate cancer–stroma interactions and a gyratory shaker to create fluid flow stimulation. Adipose–related cells, monocytes, and fluid flow influenced the proliferative potential and invasive capacity of RCC cells. Extracellular signal–regulated kinase and p38 signaling were regulated either synergistically or independently by both fluid flow and cellular interactions between RCC and adipose tissue fragments or macrophages. Fluid flow stimulation synergistically enhanced the anti–proliferative effect of sunitinib on RCC cells, but macrophages abolished the synergistic anti–proliferative effect related to fluid flow stimulation. In conclusion, we established a reconstructed model to investigate the cellular and physical microenvironments of RCC *in vitro*. Our alternative culture model may provide a promising tool for further therapeutic investigations into many types of cancer.

Keywords: clear cell renal cell carcinoma; cancer microenvironment; adipocyte; macrophage; sunitinib

Received 27 June 2020; Revised 2 November 2020; Accepted 15 January 2021

No conflicts of interest were declared.

Introduction

Renal cell carcinoma (RCC) mainly originates from the proximal convoluted tubules and accounts for 85% of renal cancer cases in the United States [1]. Clear cell renal cell carcinoma (ccRCC) is a major histological subtype of RCC that is associated with poor clinical outcomes. Forty percent of patients with ccRCC develop tumor metastases, and their 5-year survival rate is circa 10% [2]. Previous epidemiological studies demonstrated that obesity is a major risk factor for RCC [3,4]. In addition, elevated body mass index in both men and women and abdominal obesity in women may play an important role in the carcinogenesis and homeostasis of RCC [5–7].

The microenvironment includes both cellular and physical factors, and it regulates the homeostasis and function of both normal and tumor cells. For example, cell–cell interactions and the surrounding physical stimuli cooperate to form a specific microenvironment. The kidney is surrounded by perirenal adipose tissue (Figure 1A). Macrophage infiltration commonly occurs in many types of tumor, including RCC. Tumor-surrounding adipose tissue and tumor-associated macrophages (TAMs) are major components of the RCC cellular microenvironment [8,9] (Figure 1B). RCC has a highly elaborate microvasculature network that generates interstitial fluid flow, which is the movement of fluid through the extracellular compartments of tissues (Figure 1C). Therefore, from the histopathological viewpoint, adipose tissue, macrophages, and fluid flow all contribute to the RCC microenvironment.

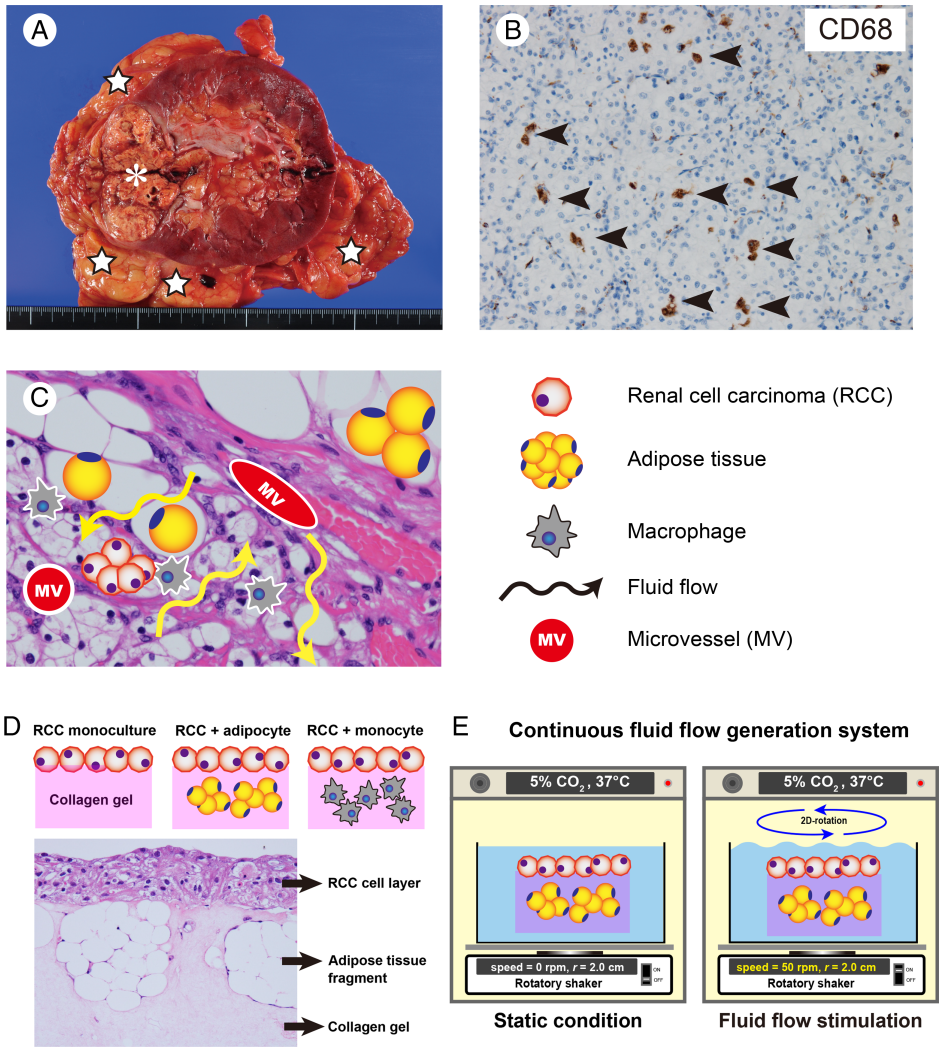

Figure 1. Specific microenvironments in RCC and experimental design. (A) Overall appearance of RCC. The kidney is surrounded by adipose tissue and Gerota's fascia. Asterisks indicate RCC; stars indicate perirenal adipose tissue. (B) CD68-positive macrophages (arrowheads) infiltrate into RCC. (C) The kidney is surrounded by perirenal adipose tissue. RCC cells are located close to adipose tissue. The abundant capillary network continuously produces interstitial fluid flow in the RCC. (D) Representative image showing the collagen gel culture model. RCC cells were seeded on collagen gel discs embedded with adipocytes or monocytes. As a control, cancer cells were seeded on collagen gel discs without adipose tissue fragments. (E) Culture dishes were placed on a rotatory shaker in a CO_2 incubator to generate fluid flow.

Previously, our group demonstrated that adipose tissue regulated the homeostasis and function of normal renal tubules [10]. Other groups, as well as our team, reported that fluid flow stimulation is a critical microenvironmental factor for various cell types, including cancer cells [11–13]. Cancer-associated adipocytes have recently been recognized as an important cellular regulator of the malignant potential of different types of cancer. In addition, previous studies have shown that both mesenchymal cells and fluid flow stimulation were key modulators of the response to molecular targeted therapy [14]. Sunitinib is a multi-targeted tyrosine kinase inhibitor that selectively inhibits several growth factor receptors, including vascular endothelial growth factor receptor 1 (VEGFR1), VEGFR2, VEGFR3, platelet-derived growth factor receptor α (PDGFR α), and PDGFR β. We selected sunitinib as the study drug for the present research because the National Comprehensive Cancer Network guideline lists sunitinib as a category 1 option for the first-line treatment of patients with relapsed or medically unresectable RCC with predominantly clear cell histology [15–17]. The interaction between the tumor microenvironment and tumor sensitivity to a molecularly targeted therapy has not been investigated for ccRCC. Therefore, this study aimed to determine the impact of cell–cell interactions and interstitial fluid flow stimulation on the kinetics of ccRCC cells and their sensitivity to sunitinib.

Materials and methods

Cells and tissue samples

All procedures involving human or animal materials were performed in accordance with the ethical guidelines of Saga University. Cells were cultured in RPMI-1640 medium (Fujifilm, Tokyo, Japan) containing 10%

fetal bovine serum (FBS), 100 μg/ml streptomycin, and 100 μg/ml penicillin. The culture medium was changed every 2 days. All cells were grown at 37 °C in 5% CO_2. The ccRCC cell line KMRC-1 (JCRB1010) with *VHL* gene mutation, the human ccRCC cell line Caki-1 (JCRB0801) with wild-type *VHL*, and the human RCC cell line VMRC-RCW (JCRB0813) were used. These three cell lines were obtained from the Japanese Cancer Research Bank (JCRB, Osaka, Japan). The human monocyte cell lines THP-1 (JCRB0112.1) and U-937 (JCRB9021) were also obtained from the JCRB. Adipose tissue fragments (ATFs) were isolated from the subcutaneous adipose tissue of 1-week-old Wistar rats. The 3T3-L1 adipocyte cell line (JCRB9014) was induced to a differentiated state with conventional protocols [18]. Our previous studies have addressed the issue of species differences in humoral cross-reactivity and confirmed that rat-derived adipose tissue exhibits cross-reactivity with human-derived cells [11,14].

Cell culture model

We used a collagen gel culture method to analyze the cell–cell interactions between RCC cells and stromal cells (Figure 1D). First, 0.2 g of ATFs, 2.0×10^5 adipocytes differentiated from 3T3-L1 cells or 2.0×10^5 monocytes (THP-1 cells or U-937 cells) were embedded in a collagen disc (Cellmatrix, Type I-A; Nitta Gelatin, Osaka, Japan). Subsequently, 2.0×10^5 RCC cells (KMRC-1, Caki-1 or VMRC-RCW) were seeded onto the surface of the collagen disc. After overnight incubation, the collagen gel discs were transferred to 10-cm dishes with 20 ml of culture medium. In the control monoculture group, RCC cells were seeded on collagen gel discs without stromal cells (Figure 1D). After 7 days of culture, tissues were fixed with 10% formalin and embedded in paraffin.

Fluid flow-generating system

The fluid flow-generating system has been reported in our previous study [19]. Samples were incubated in 5% CO_2 and 20% O_2 at 37 °C in a CO_2 incubator. To generate fluid flow, the culture dishes were placed on a rotatory shaker (MIR-S100C; Panasonic, Tokyo, Japan) at 50 rpm throughout the culture period. Control dishes were placed in the same CO_2 incubator under static conditions (Figure 1E). Fluid flow magnitude is an important factor regulating cellular kinetics, and we have previously confirmed that a rotation speed of 40–50 rpm is suitable for cells grown on the surface of a collagen disc.

Immunohistochemistry

Histological examinations were performed in hematoxylin and eosin (H&E)-stained sections. Cell proliferation was analyzed using a mouse monoclonal anti-proliferating cell nuclear antigen (PCNA) antibody (M0879; Dako, Glostrup, Denmark). Cell apoptosis was evaluated using anti-cleaved caspase 3 antibody [#9664; Cell Signaling Technology (CST), Danvers, MA, USA]. Immunostaining for PCNA and cleaved caspase 3 was detected using Histofine® Simple Stain MAX PO (Nichirei, Tokyo, Japan). Immunofluorescence analyses were carried out using anti-VEGF primary antibody (19003-1-AP; Proteintech, Rosemont, IL, USA), anti-PDGFRβ primary antibody (#3169; CST), and Alexa Fluor 488-conjugated secondary antibody (A32731; Invitrogen, Carlsbad, CA, USA). Images were analyzed with an Axio Imager 2 light microscope and ApoTome.2 system (Carl Zeiss, Oberkochen, Germany).

Morphometric analysis

Cells were counted in five randomly selected non-contiguous and non-overlapping fields within the stained sections, and the percentages of PCNA-positive cells and cleaved caspase 3-positive cells were determined to evaluate proliferation and apoptosis, respectively. Cancer layer thicknesses were measured at six points in all five randomly selected non-contiguous and non-overlapping areas (low magnification, ×10 objective).

Western blotting and protein array analysis

KMRC-1 cells, ATFs, and THP-1 cells were co-cultured using inserts with an 8-μm pore size (Falcon Cell Culture Insert; Becton Dickinson, Franklin, NJ, USA) to prepare protein lysates. ATFs and THP-1 cells were embedded in collagen gels, and KMRC-1 cells were seeded on collagen gels. The inserts were placed in 10-cm dishes with 20 ml of complete medium. After 72 h of culture, the collagen gels were stripped from the inserts. KMRC-1 cells were lysed in 400 μl of M-PER Reagent (Thermo Fisher Scientific, Waltham, MA, USA) supplemented with a protease–phosphatase inhibitor cocktail (CST). Lysates were incubated at 95 °C for 10 min, and then 20 μl of each sample was loaded onto a 4% sodium dodecyl sulfate-containing polyacrylamide gel (Bio-Rad Laboratories, Hercules, CA, USA). Blotted membranes were incubated overnight at 4 °C with antibodies raised against extracellular signal-regulated kinase (ERK) 1/2 (#9102; CST), p-ERK1/2 (#4370; CST), p38 (#8690; CST), p-p38 (#4511; CST), CD68 (M0718; Dako), CD163 (16646-1-AP; Proteintech), and CD11c (17342-1-AP; Proteintech). Antibody-bound antigens on the membranes were detected with a chemiluminescent immunodetection system (Western Breeze; Thermo Fisher Scientific). The band densities were measured using a FUSION system (Vilber-Lourmat, Eberhardzell, Germany) and analyzed with ImageJ software [National Institutes of Health (NIH), Bethesda, MD, USA].

A proteome profiler antibody array (R&D Systems, Abingdon, UK) was used in accordance with the manufacturer's instructions to examine cytokine receptor expression. Imaging was performed using a FUSION system (Vilber-Lourmat), and all images were analyzed using ImageJ software (NIH).

Sunitinib administration

To examine the effects of sunitinib on ccRCC cells, the culture medium was changed to new medium containing sunitinib (Tocris Bioscience, Bristol, UK) at final concentrations of 2.5, 5.0 or 10.0 ng/ml. The medium was changed every 2 days, and the samples were collected and analyzed at day 7.

Statistical analysis

The mean values of replicates were compared between groups using unpaired two-tailed *t*-tests and Tukey's HSD tests. $p < 0.05$ was considered to indicate a statistically significant difference. All statistical analyses were performed using SPSS 23 (IBM Corp, Armonk, NY, USA).

Results

The cellular and physical microenvironments synergistically regulate the cellular behavior of RCC

To clarify the effects of cell–cell interactions on RCC, we cultured three different RCC cell lines on the surfaces of collagen gel discs containing various stromal cell types (ATFs, 3T3-L1 adipocytes or monocytes). Under static conditions, KMRC-1 cells, Caki-1 cells, and VMRC-RCW cells exhibited a flat cytoplasm with a two- to three-layer structure when cultured in the absence of any cancer-associated cells or in the presence of monocytes (THP-1 cells or U-937 cells) (Figure 2 and supplementary material, Table S1). By contrast, all three RCC lines exhibited cytoplasmic hypertrophy, an increased nuclear–cytoplasmic ratio, and a thickened stratified layer structure when cultured with adipose-related cells (ATFs or 3T3-L1 cells).

Next, the cultured discs were incubated under fluid flow stimulation to evaluate the effects of the physical microenvironment on RCCs. RCC cell lines cultured with or without cancer-associated cells exhibited increased cell numbers, cytoplasmic hypertrophy, and significant thickening of the cellular layers under fluid flow stimulation, compared with static conditions. Adipose-related cells (ATFs and 3T3-L1 cells) significantly enhanced the thickening of the KMRC-1 cellular layer under fluid flow stimulation compared with the other groups. The thicknesses of the cellular layers in the various groups under static and fluid flow conditions are listed in supplementary material, Table S1. Notably, fluid flow stimulation induced the invasion of KMRC-1 cells and Caki-1 cells into the ATFs.

The cellular and physical microenvironments synergistically affect the growth and survival of RCC

The percentages of PCNA-positive KMRC-1 cells and Caki-1 cells in the various experimental groups under static conditions and fluid flow conditions are presented in supplementary material, Table S2. Monocytes did not affect the growth of KMRC-1 cells. Under static conditions, the number of PCNA-positive KMRC cells was significantly higher after co-culture with adipose-related cells than after co-culture with monocytes (Figure 3 and supplementary material, Table S2). Under static conditions, the number of PCNA-positive Caki-1 cells was significantly lower for cells co-cultured with THP-1 cells than for cells in monoculture, and this inhibitory effect of THP-1 cells on the proliferation of Caki-1 cells was abolished under fluid flow stimulation.

The percentages of cleaved caspase 3-positive Caki-1 cells in the various groups under static and fluid flow conditions are listed in supplementary material, Table S2. Under static conditions, 3T3-L1 cells increased the number of cleaved caspase 3-positive Caki-1 cells. Under fluid flow conditions, there were no significant differences in the number of cleaved caspase 3-positive Caki-1 cells between the various groups. However, the number of cleaved caspase 3-positive Caki-1 cells differed significantly between static conditions and fluid flow conditions.

The cellular and physical microenvironments modulate the expression of VEGF and PDGFR

As shown in Figure 4, immunostaining for VEGF and PDGFR in the RCC cell monoculture group demonstrated weak positivity under static conditions and a slight enhancement of the staining intensity for VEGF and PDGFR under fluid flow stimulation. Under static conditions, ATFs slightly increased the staining intensity for VEGF in KMRC-1 cells, whereas 3T3-L1 cells, THP-1 cells, and U-937 cells did not affect the staining intensity for VEGF and PDGFR in KMRC-1 cells. Under fluid flow stimulation, ATFs and THP-1 cells enhanced the VEGF staining intensity in RCC cells compared with the other monoculture and co-culture groups. Furthermore, the staining intensities for VEGF and PDGFR in RCC cells co-cultured with 3T3-L1 cells or U-937 cells were greater under fluid flow conditions than under static conditions.

The cellular and physical microenvironments affect mitogen-activated protein kinase (MAPK) signaling in ccRCC

MAPK pathways are involved in the proliferation and migration of ccRCC [20]. To investigate the effect of the microenvironment on the cellular kinetics of ccRCC, we evaluated ERK1/2 and p38 expression in KMRC cells cultured in the presence of stromal or immune cells under static conditions or fluid flow stimulation. As shown in Figure 5, total ERK1/2 and p38 expression was higher in KMRC-1 cells cultured with ATFs than in KMRC-1 cells co-cultured with THP-1 cells under static conditions. The phosphorylated-to-total ERK1/2 ratio was higher for KMRC-1 cells co-cultured with THP-1 cells than for cells in monoculture under static conditions. Additionally, compared with static conditions, fluid flow stimulation upregulated total ERK1/2

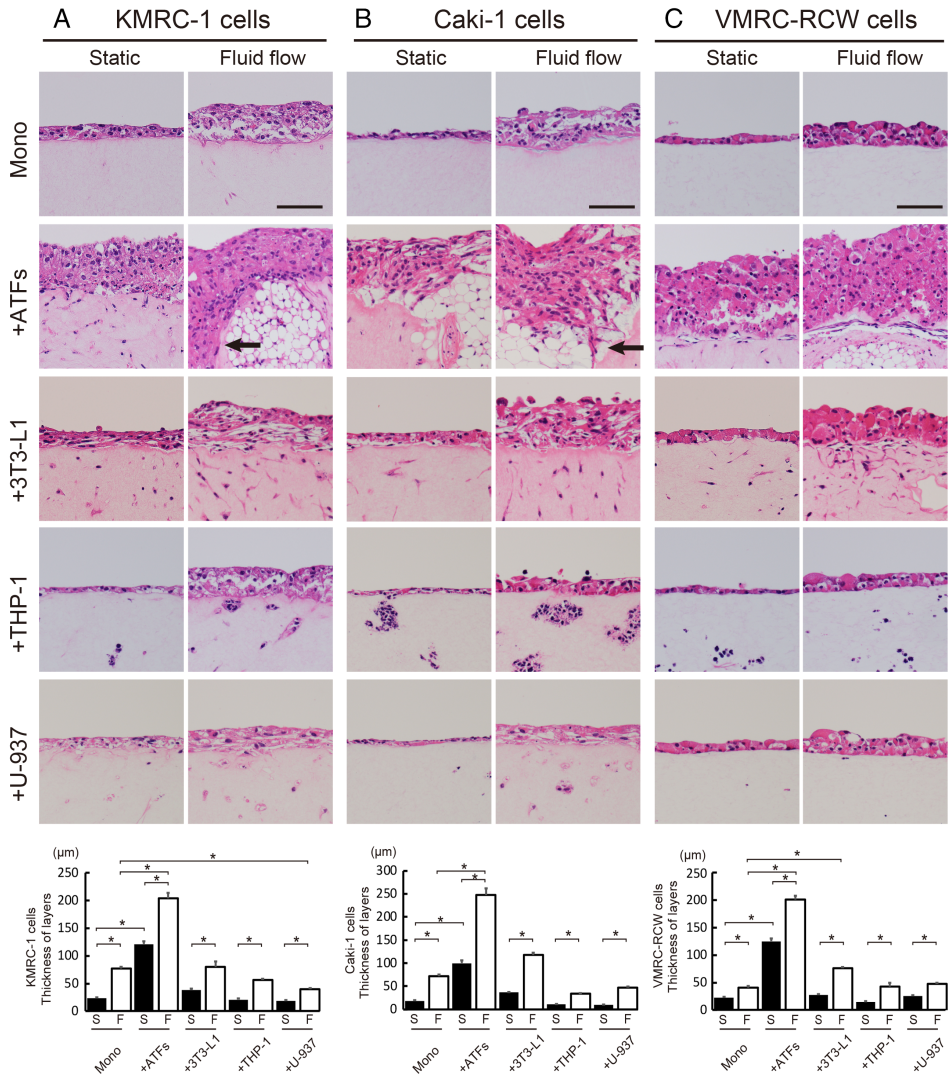

Figure 2. Fluid flow and stromal cells affect the cellular kinetics of RCC. Representative images at day 7. RCC cells cultured with THP-1 cells or U-937 cells had a flat cytoplasm and a two- to three-layered structure. Fluid flow acted synergistically with ATFs or 3T3-L1 cells to promote cellular hypertrophy and thickening of the epithelial layer of RCC cells. KMRC-1 cells and Caki-1 cells had invaded the adipose tissue (arrowhead). Mean ± SEM of three determinations. *$p < 0.05$. Mono, cultured without cancer-associated cells; ATFs, adipose tissue fragments. Bar = 50 μm.

and p38 expression in KMRC-1 cells co-cultured with THP-1 cells.

The cellular and physical microenvironments modulate the sensitivity of ccRCC to sunitinib

We evaluated the sensitivity of KMRC-1 cells to various concentrations (2.5, 5.0, and 10.0 ng/ml) of sunitinib (Figure 6A). Under static conditions, 5.0 and 10.0 ng/ml sunitinib significantly reduced the thickness of KMRC-1 cellular layers compared with the control group. As described above, fluid flow stimulation increased the thickness of KMRC-1 cellular layers. Furthermore, fluid flow enhanced the anti-proliferative action of sunitinib on KMRC-1 cells, even in cells treated with 2.5 ng/ml sunitinib, compared with the control group. Next, we examined the effects of 5.0 ng/ml sunitinib on KMRC-1 cells under monoculture and co-culture conditions (Figure 6B). Under static conditions, ATFs and THP-1 cells did not affect the thickness of KMRC-1 cellular layers compared with the monoculture group. Notably, fluid flow stimulation promoted the anti-proliferative effect of sunitinib on KMRC-1 cells in monoculture and in co-culture with ATFs, but THP-1 cells abolished the enhancement of sunitinib's anti-proliferative action by fluid flow stimulation. Following sunitinib administration, THP-1 cells upregulated total ERK1/2 expression and decreased the phosphorylated-to-total ERK1/2 ratio in KMRC-1 cells compared with the group co-cultured with ATFs under fluid flow stimulation (Figure 6C). Sunitinib significantly decreased the phosphorylated-to-total p38 ratio in KMRC-1 cells in monoculture under static conditions. Sunitinib had no effects on total p38 expression in KMRC-1 cells in any of the groups (monoculture or co-culture, static conditions or fluid flow conditions).

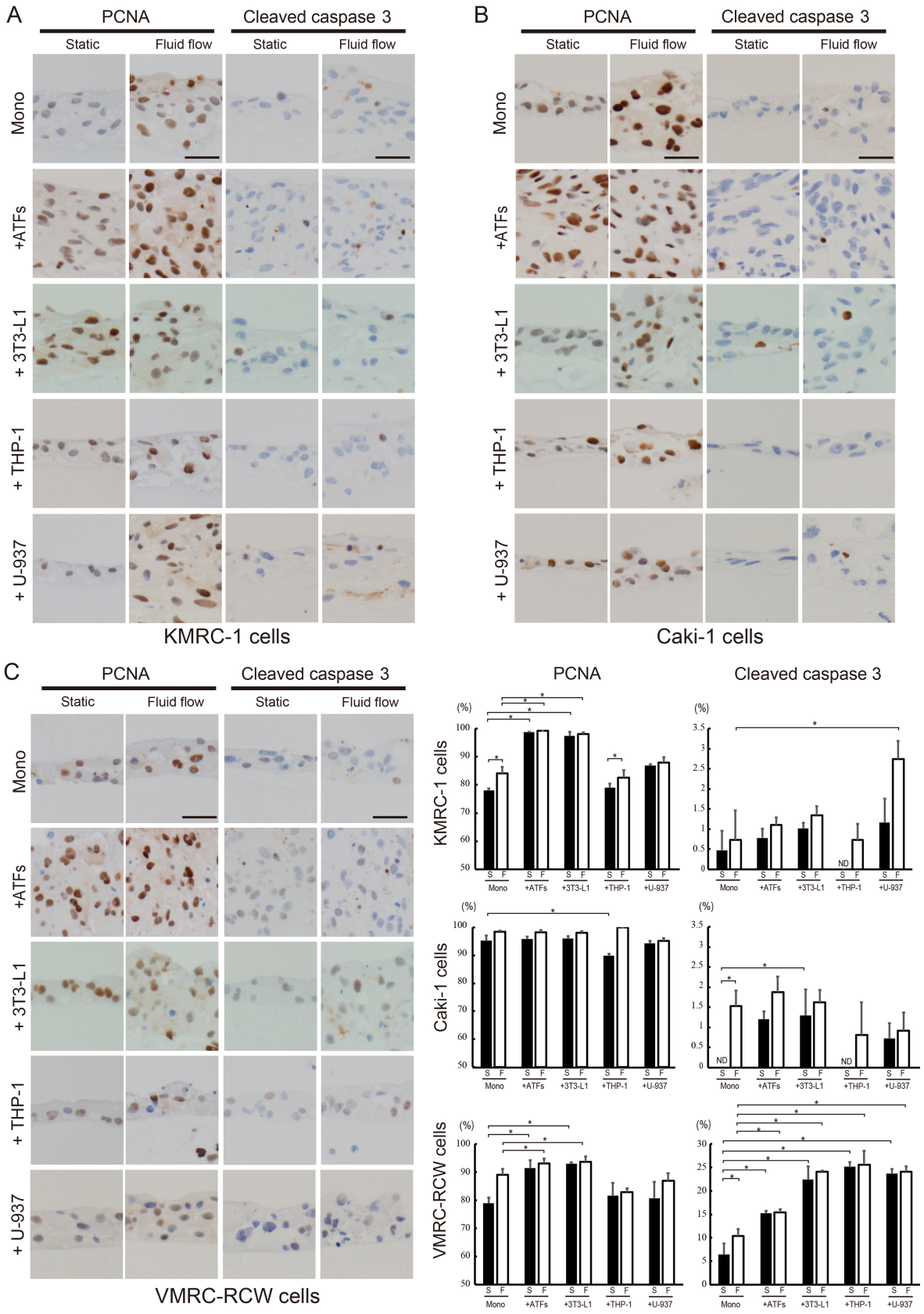

Figure 3. Fluid flow and stromal cells modulate the proliferation and apoptosis of RCC. Representative images showing immunostaining of PCNA and cleaved caspase 3 in KMRC-1 cells, Caki-1 cells, and VMRC-RCW cells at day 7. Fluid flow itself increased the number of PCNA-positive RCC cells. Fluid flow and stromal cell types acted synergistically to modulate the proliferation and apoptosis of RCC. *$p < 0.05$. Mono, cultured without cancer-associated cells; ATFs, adipose tissue fragments.

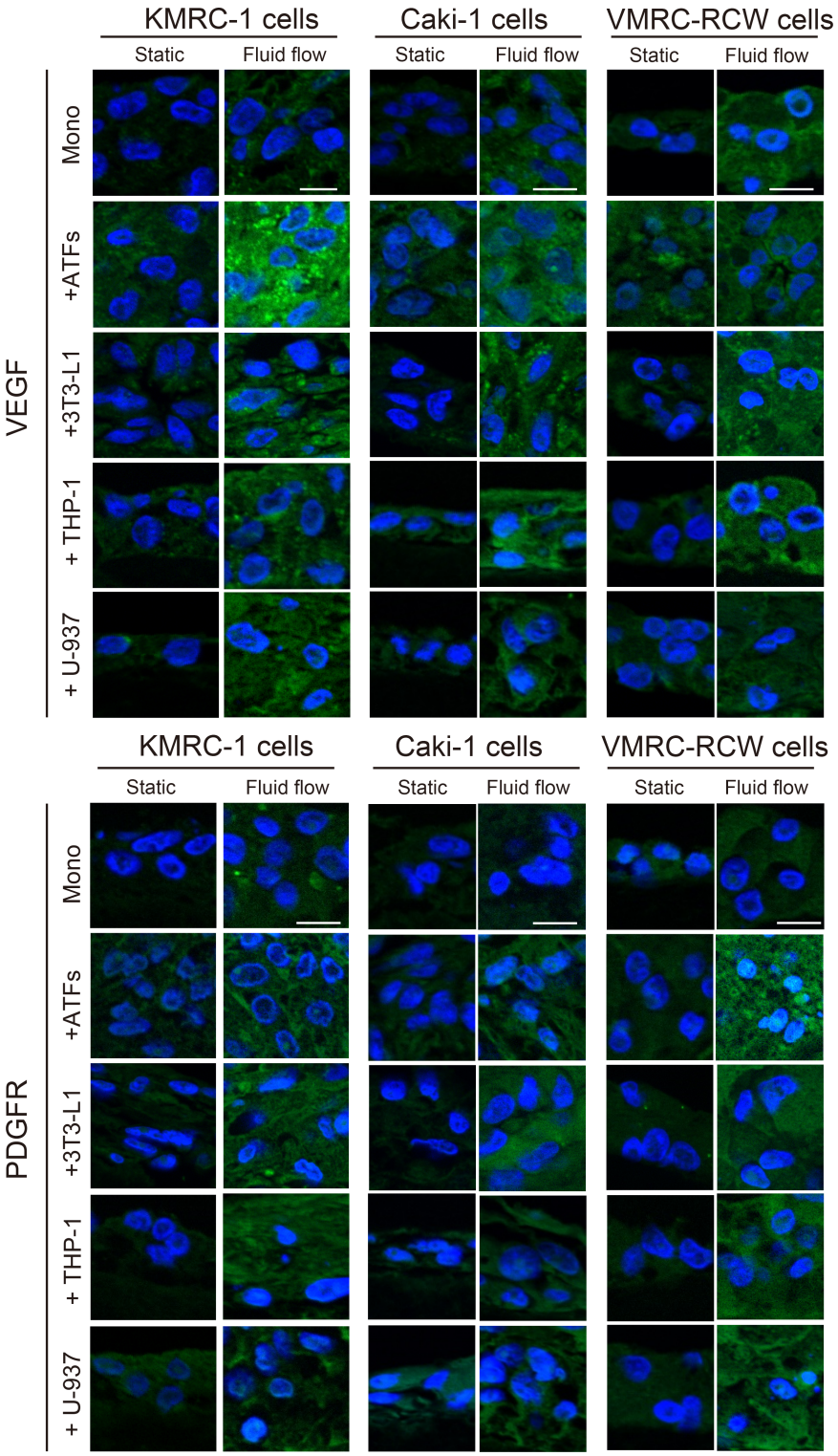

Figure 4. Effects of stromal cells and fluid flow on VEGF and PDGFR expression in RCC. Representative images showing immunostaining for VEGF and PDGFR in RCC cells (VEGF or PDGFR immunofluorescence is shown in green and staining of nuclei by DAPI is shown in blue). VEGF and PDGFR expression was increased under fluid flow conditions compared with static conditions. The levels of VEGF and PDGFR expression were greater in RCCs co-cultured with ATFs than in RCCs co-cultured with 3T3-L1 cells. Mono, cultured without cancer-associated cells; ATFs, adipose tissue fragments. Bar = 10 μm.

THP-1 cells exhibited a CD11c-positive phenotype when co-cultured with KMRC-1 cells

The M1/M2 ratio of tumor-associated macrophages is an important regulator of and prognostic factor for various cancers including RCC [21–23]. Therefore, we determined the M1/M2 ratio using western blotting to evaluate the M1 macrophage marker CD11c and the M2 macrophage marker CD163 [24]. THP-1 showed negative expression of CD11c and CD163 under static conditions

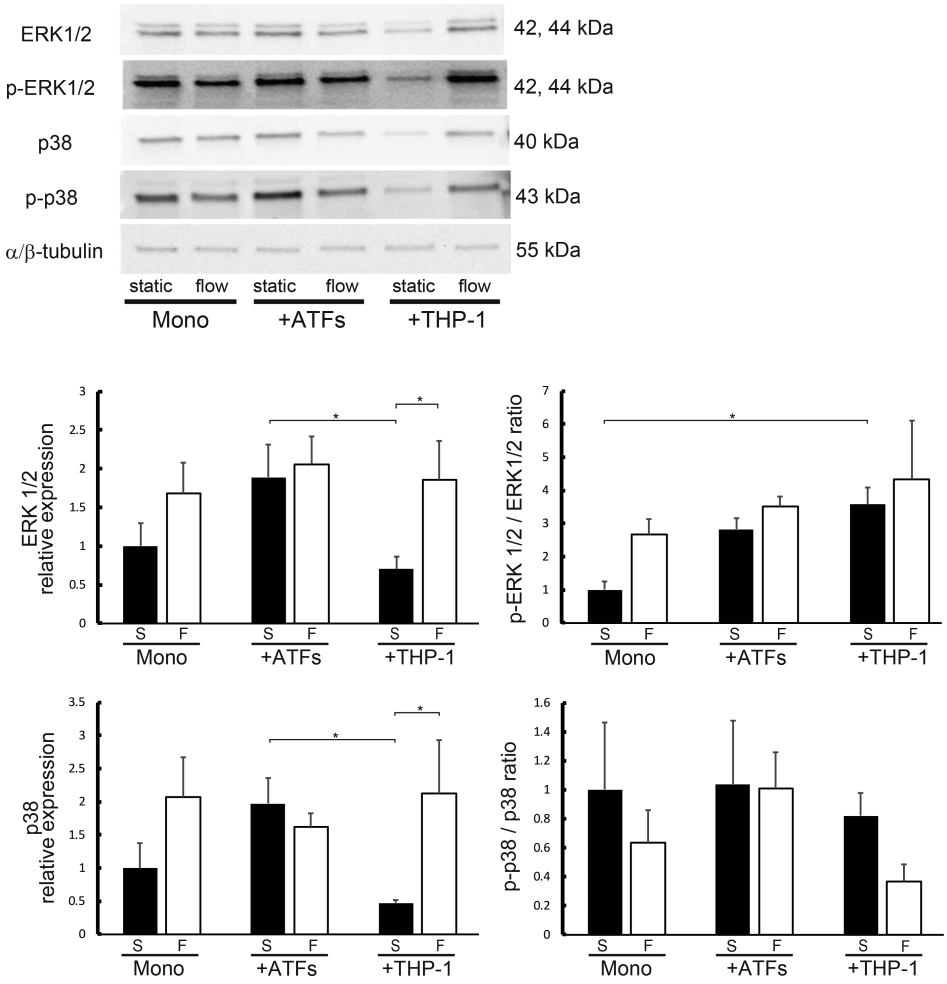

Figure 5. Effects of stromal cells and fluid flow on MAPK signaling in RCC. ERK1/2, p-ERK1/2, p38, and p-p38 expression in KMRC-1 cells evaluated by western blotting. Relative expression levels are shown as the ratio of the target protein expression to α/β-tubulin expression. Mean ± SD of 3–5 determinations. *$p < 0.05$. Mono, cultured without cancer-associated cells; ATFs, adipose tissue fragments; S, static; F, fluid flow.

and fluid flow conditions both in the absence and in the presence of sunitinib. In contrast, THP-1 cells co-cultured with KMRC-1 cells expressed CD11c under static and fluid flow conditions both in the absence and in the presence of sunitinib (supplementary material, Figure S1).

Discussion

In the present study, we used a novel three-dimensional culture system to demonstrate that two characteristics of the microenvironment (i.e. interactions between cells and fluid flow stimulation) synergistically regulated the behavior of ccRCC. Recently, numerous studies have demonstrated that the cellular microenvironment plays a pivotal role in the invasion and growth of tumors [24]. The major cellular microenvironment of ccRCC is composed of adipose tissue and macrophages. In the presence of cancer, adipose tissue and macrophages function as cancer-associated adipocytes and TAMs, respectively [25–28]. Cancer-associated adipocytes are recognized as important factors driving cancer progression [29,30]. However, our study revealed that adipose tissue accelerated the invasive capacity of ccRCC only under fluid flow stimulation. In addition, adipose tissue did not accelerate the proliferative capacity of ccRCC under static or fluid flow conditions. These results suggest that fluid flow is a growth-stimulating factor for ccRCC and might promote the infiltration of adipose tissue by ccRCC.

The dense infiltration of TAMs in cancer tissues is known to correlate strongly with a poor prognosis [31,32]. However, several reports have demonstrated that ccRCC attracts macrophages and induces monocyte differentiation into CD163-positive macrophages [33,34] and that CD11c-positive macrophages produce cytotoxic mediators and/or chemokines involved in tumor suppression and immune stimulation [35,36]. Similar to previous reports, our findings support an anti-proliferative effect of CD11c-positive macrophages on ccRCC. Moreover, our results suggest that CD11c-positive macrophages may suppress the sensitivity of ccRCC cells to sunitinib under fluid flow conditions (supplementary material, Figure S1).

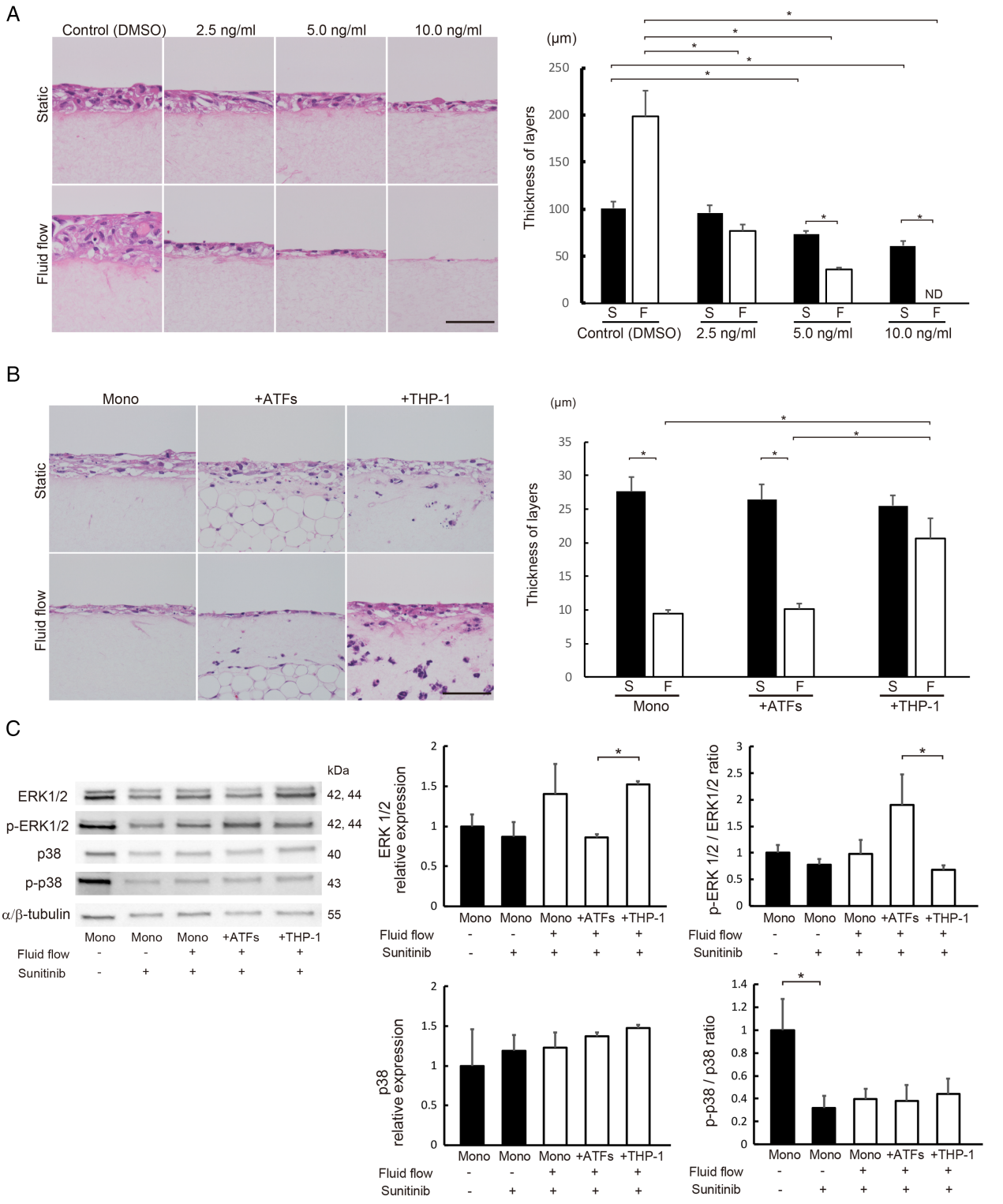

Figure 6. Effects of stromal cells and fluid flow on the chemosensitivity of RCC cells to sunitinib. (A) Alterations in the morphology and cellular layer thickness of KMRC-1 cells at day 7 after treatment with 2.5, 5.0 or 10.0 ng/ml sunitinib. (B) Representative images showing the cellular layer thickness of KMRC-1 cells in the monoculture group and co-culture groups (with ATFs or THP-1 cells) at day 7. (C) ERK1/2, p-ERK1/2, p38, and p-p38 expression levels in KMRC-1 cells following the administration of 5.0 ng/ml sunitinib were evaluated by western blotting. Relative expression was calculated as the ratio of the target protein expression to α/β-tubulin expression. Mean ± SD of 3–5 determinations. $^*p < 0.05$. Mono, cultured without cancer-associated cells; ATFs, adipose tissue fragments; S, static; F, fluid flow; ND, not detected.

Therefore, the unexpected effect of CD11c-positive macrophages on sunitinib sensitivity identified in our study may be affected by the physical environment around the tumor.

The physical microenvironment, especially fluid flow, is a critical regulatory factor for various cells including cancer cells [11,14,37]. However, the importance of physical stimulation on the cellular kinetics of ccRCC

is poorly understood. RCC has a highly elaborate microvascular network that generates fluid flow stimulation in tumors composed of cancer cells and associated cells. Moreover, the effect of physical stimulation on cell–cell interactions is not fully understood. As described above, our study clearly demonstrated that fluid flow stimulation modifies the effect of the cellular microenvironment not only on cancer cells but also on tumor-associated cells. The inhibitory effect of monocytes on the drug sensitivity of RCC was influenced by fluid flow. Therefore, it will be important to characterize stromal alterations (such as changes in the cell phenotype and extracellular matrix) that are induced by physical stimulation. The mechanisms underlying the relationship between flow stimulation and drug sensitivity remain uncharacterized. We observed that fluid flow promotes the diffusion of small particles (data not shown), but Santoro *et al* reported that biomechanical stimulation due to flow perfusion can affect the drug sensitivity of sarcoma [38]. These findings suggest that both diffusion and mechanical stimulation may mediate the effects of fluid flow on the sensitivity of RCC to sunitinib. Further studies are needed to better understand the impact of fluid flow and to explore the biological link between cellular and physical microenvironments as a potential target for new cancer treatment strategies.

The *VHL* gene is inactivated in ccRCC, and the α subunit of hypoxia-inducible factor (HIF) is subsequently constitutively stabilized. Therefore, VEGF overexpression and exacerbated vascularization likely occur in ccRCC. KMRC-1 cells cultured with ATFs or THP-1 cells exhibited high expression of VEGF and PDGFR, suggesting that ATFs and THP-1 cells may increase VEGF and PDGFR expression under fluid flow conditions and thereby enhance cell growth and proliferation. Because VEGF is related to MAPK signaling, we evaluated the effects of sunitinib on this signaling pathway [39–41]. As shown in Figure 6C, sunitinib inhibited the phosphorylation of ERK1/2 in KMRC-1 cells cultured with THP-1 cells. In contrast, sunitinib did not affect the levels of total or phosphorylated p38 in KMRC-1 cells. A recent study suggested that sunitinib inhibited signal transducer and activator of transcription 3 (STAT3) signaling in ccRCC [42]. A related study established crosstalk between STAT3 and MAPK signaling pathways, particularly ERK1/2 [43]. Therefore, it is possible that sunitinib inhibits ERK1/2 via STAT3, but further studies are needed to confirm this hypothesis. It should also be recognized that sunitinib targets signaling pathways other than MAPK. Sunitinib is a multi-target kinase inhibitor that affects receptor tyrosine kinases such as VEGFRs, PDGFRs, stem cell factor receptor, FMS-like tyrosine kinase-3, glial cell line-derived neurotrophic factor receptor, and the receptor of macrophage colony-stimulating factor [44]. These other signaling pathways targeted by sunitinib are critical regulators of RCC behavior, and further studies are needed to establish their relevance to our findings.

In conclusion, we have established a reconstructed model that mimics the cellular and physical microenvironment of ccRCC *in vitro*. Each cellular or physical factor is an independent or coordinated integral component that regulates the malignant potential and drug sensitivity of cancer cells. Our novel alternative *in vitro* model may be a promising tool to facilitate therapeutic investigations in many types of cancer.

Acknowledgements

We thank T Sakumoto, M Nishida, F Mutoh, S Nakahara and I Nanbu for their excellent technical assistance. This work was supported in part by a Grant-in-Aid from the Japanese Ministry of Education, Culture, Sports, Science and Technology for Scientific Research (No 2546170 to SA) and personal grants from Shunan Memorial Hospital.

Author contributions statement

KN and SA conceived and designed the project. KN, TA, MR, SM, MF and SA performed the experiments. KN, SA, ST, MN and ST interpreted and analyzed the data. KN and SA wrote the manuscript. All the authors revised the paper and approved the final submitted version.

References

1. Kumar V, Abbas AK, Fausto N, *et al*. *Robbins and Cotran Pathologic Basis of Disease,* Professional Edition E-Book. Elsevier Health Sciences, 2014.
2. Heidegger I, Pircher A, Pichler R. Targeting the tumor microenvironment in renal cell cancer biology and therapy. *Front Oncol* 2019; **9:** 490.
3. Washio M, Mori M, Mikami K, *et al*. Risk factors for renal cell carcinoma in a Japanese population. *Asian Pac J Cancer Prev* 2014; **15:** 9065–9070.
4. Chow W-H, Gridley G, Fraumeni JF Jr, *et al*. Obesity, hypertension, and the risk of kidney cancer in men. *N Engl J Med* 2000; **343:** 1305–1311.
5. Lipworth L, Tarone RE, Lund L, *et al*. Epidemiologic characteristics and risk factors for renal cell cancer. *Clin Epidemiol* 2009; **1:** 33–43.
6. Rajandram R, Perumal K, Yap NY. Prognostic biomarkers in renal cell carcinoma: is there a relationship with obesity? *Transl Androl Urol* 2019; **8:** S138–S146.
7. Campo-Verde-Arbocco F, López-Laur JD, Romeo LR, *et al*. Human renal adipose tissue induces the invasion and progression of renal cell carcinoma. *Oncotarget* 2017; **8:** 94223–94234.
8. Buoncervello M, Gabriele L, Toschi E. The Janus face of tumor microenvironment targeted by immunotherapy. *Int J Mol Sci* 2019; **20:** 4320.
9. Ma C, Komohara Y, Ohnishi K, *et al*. Infiltration of tumor-associated macrophages is involved in CD44 expression in clear cell renal cell carcinoma. *Cancer Sci* 2016; **107:** 700–707.
10. Udo K, Aoki S, Uchihashi K, *et al*. Adipose tissue explants and MDCK cells reciprocally regulate their morphogenesis in coculture. *Kidney Int* 2010; **78:** 60–68.
11. Kawata K, Aoki S, Futamata M, *et al*. Mesenchymal cells and fluid flow stimulation synergistically regulate the kinetics of corneal epithelial cells at the air–liquid interface. *Graefes Arch Clin Exp Ophthalmol* 2019; **257:** 1915–1924.

12. Aoki S, Makino J, Nagashima A, *et al*. Fluid flow stress affects peritoneal cell kinetics: possible pathogenesis of peritoneal fibrosis. *Perit Dial Int* 2011; **31:** 466–476.
13. Mitchell MJ, King MR. Computational and experimental models of cancer cell response to fluid shear stress. *Front Oncol* 2013; **3:** 44.
14. Akutagawa T, Aoki S, Yamamoto-Rikitake M, *et al*. Cancer–adipose tissue interaction and fluid flow synergistically modulate cell kinetics, HER2 expression, and trastuzumab efficacy in gastric cancer. *Gastric Cancer* 2018; **21:** 946–955.
15. Mendel DB, Laird AD, Xin X, *et al*. *In vivo* antitumor activity of SU11248, a novel tyrosine kinase inhibitor targeting vascular endothelial growth factor and platelet-derived growth factor receptors: determination of a pharmacokinetic/pharmacodynamic relationship. *Clin Cancer Res* 2003; **9:** 327–337.
16. Motzer RJ, Agarwal N, Beard C, *et al*. Kidney cancer. *J Natl Compr Canc Netw* 2009; **7:** 618–630.
17. Gulati S, Vaishampayan U. Current state of systemic therapies for advanced renal cell carcinoma. *Curr Oncol Rep* 2020; **22:** 26.
18. Zebisch K, Voigt V, Wabitsch M, *et al*. Protocol for effective differentiation of 3T3-L1 cells to adipocytes. *Anal Biochem* 2012; **425:** 88–90.
19. Aoki S, Ikeda S, Takezawa T, *et al*. Prolonged effect of fluid flow stress on the proliferative activity of mesothelial cells after abrupt discontinuation of fluid streaming. *Biochem Biophys Res Commun* 2011; **416:** 391–396.
20. Huang B, Fu SJ, Fan WZ, *et al*. PKCε inhibits isolation and stemness of side population cells via the suppression of ABCB1 transporter and PI3K/Akt, MAPK/ERK signaling in renal cell carcinoma cell line 769P. *Cancer Lett* 2016; **376:** 148–154.
21. Ahmad S, Singh V, Sinha RJ, *et al*. Role of MMP-2, MMP-9 and VEGF as serum biomarker in early prognosis of renal cell carcinoma. *Afr J Urol* 2018; **24:** 255–263.
22. Caux C, Ramos RN, Prendergast GC, *et al*. A milestone review on how macrophages affect tumor growth. *Cancer Res* 2016; **76:** 6439–6442.
23. Chen SJ, Yao XD, Peng BO, *et al*. Epigallocatechin-3-gallate inhibits migration and invasion of human renal carcinoma cells by downregulating matrix metalloproteinase-2 and matrix metalloproteinase-9. *Exp Ther Med* 2016; **11:** 1243–1248.
24. Thakkar S, Sharma D, Kalia K, *et al*. Tumor microenvironment targeted nanotherapeutics for cancer therapy and diagnosis: a review. *Acta Biomater* 2020; **101:** 43–68.
25. Wu Q, Li B, Li Z, *et al*. Cancer-associated adipocytes: key players in breast cancer progression. *J Hematol Oncol* 2019; **12:** 95.
26. Santoni M, Massari F, Amantini C, *et al*. Emerging role of tumor-associated macrophages as therapeutic targets in patients with metastatic renal cell carcinoma. *Cancer Immunol Immunother* 2013; **62:** 1757–1768.
27. Chávez-Galán L, Olleros ML, Vesin D, *et al*. Much more than M1 and M2 macrophages, there are also $CD169^+$ and TCR^+ macrophages. *Front Immunol* 2015; **6:** 263.
28. Fujisaka S, Usui I, Ikutani M, *et al*. Adipose tissue hypoxia induces inflammatory M1 polarity of macrophages in an HIF-1α-dependent and HIF-1α-independent manner in obese mice. *Diabetologia* 2013; **56:** 1403–1412.
29. Laurent V, Guérard A, Mazerolles C, *et al*. Periprostatic adipocytes act as a driving force for prostate cancer progression in obesity. *Nat Commun* 2016; **7:** 1–15.
30. Wang YY, Attané C, Milhas D, *et al*. Mammary adipocytes stimulate breast cancer invasion through metabolic remodeling of tumor cells. *JCI Insight* 2017; **2:** e87489.
31. Mantovani A, Schioppa T, Porta C, *et al*. Role of tumor-associated macrophages in tumor progression and invasion. *Cancer Metastasis Rev* 2006; **25:** 315–322.
32. Condeelis J, Pollard JW. Macrophages: obligate partners for tumor cell migration, invasion, and metastasis. *Cell* 2006; **124:** 263–266.
33. Cros J, Sbidian E, Posseme K, *et al*. Nestin expression on tumour vessels and tumour-infiltrating macrophages define a poor prognosis subgroup of pt1 clear cell renal cell carcinoma. *Virchows Arch* 2016; **469:** 331–337.
34. Ma C, Horlad H, Ohnishi K, *et al*. CD163-positive cancer cells are potentially associated with high malignant potential in clear cell renal cell carcinoma. *Med Mol Morphol* 2018; **51:** 13–20.
35. Allavena P, Mantovani A. Immunology in the clinic review series; focus on cancer: tumour-associated macrophages: undisputed stars of the inflammatory tumour microenvironment. *Clin Exp Immunol* 2012; **167:** 195–205.
36. Solinas G, Germano G, Mantovani A, *et al*. Tumor-associated macrophages (TAM) as major players of the cancer-related inflammation. *J Leukoc Biol* 2009; **86:** 1065–1073.
37. Avraham-Chakim L, Elad D, Zaretsky U, *et al*. Fluid-flow induced wall shear stress and epithelial ovarian cancer peritoneal spreading. *PLoS One* 2013; **8:** e60965.
38. Santoro M, Lamhamedi-Cherradi S-E, Menegaz BA, *et al*. Flow perfusion effects on three-dimensional culture and drug sensitivity of Ewing sarcoma. *Proc Natl Acad Sci U S A* 2015; **112:** 10304–10309.
39. Huang D, Ding Y, Luo WM, *et al*. Inhibition of MAPK kinase signaling pathways suppressed renal cell carcinoma growth and angiogenesis *in vivo*. *Cancer Res* 2008; **68:** 81–88.
40. Huang X, Huang S, Zhang F, *et al*. Lentiviral-mediated Smad4 RNAi promotes SMMC-7721 cell migration by regulation of MMP-2, VEGF and MAPK signaling. *Mol Med Rep* 2010; **3:** 295–299.
41. Milkiewicz M, Mohammadzadeh F, Ispanovic E, *et al*. Static strain stimulates expression of matrix metalloproteinase-2 and VEGF in microvascular endothelium via JNK- and ERK-dependent pathways. *J Cell Biochem* 2007; **100:** 750–761.
42. Xin H, Zhang C, Herrmann A, *et al*. Sunitinib inhibition of Stat3 induces renal cell carcinoma tumor cell apoptosis and reduces immunosuppressive cells. *Cancer Res* 2009; **69:** 2506–2513.
43. Gkouveris I, Nikitakis N, Karanikou M, *et al*. Erk1/2 activation and modulation of STAT3 signaling in oral cancer. *Oncol Rep* 2014; **32:** 2175–2182.
44. Atkins M, Jones CA, Kirkpatrick P. Sunitinib maleate. *Nat Rev Drug Discov* 2006; **5:** 279–280.

SUPPLEMENTARY MATERIAL ONLINE

Figure S1. THP-1 cells expressed CD11c when co-cultured with KMRC-1 cells

Table S1. Thicknesses of the cellular layers in each of the culture models

Table S2. Percentage of PCNA-positive cells and cleaved caspase 3-positive cells